Electromagnetics
Publication details, including instructions for authors and subscription information:
http://www.tandfonline.com/loi/uemg20

Domain Product Technique Solution for Scattering by Cylindrical Obstacle in Rectangular Waveguide

Vitaliy P. Chumachenko [a] & Igor V. Petrusenko [a]
[a] Gebze Institute of Technology Gebze, Turkey
Published online: 10 Nov 2010.

To cite this article: Vitaliy P. Chumachenko & Igor V. Petrusenko (2002) Domain Product Technique Solution for Scattering by Cylindrical Obstacle in Rectangular Waveguide, Electromagnetics, 22:6, 473-486, DOI: 10.1080/02726340290084067

To link to this article: http://dx.doi.org/10.1080/02726340290084067

Electromagnetics, 22:473–486, 2002

0272-6343/02 $12.00 + .00
DOI: 10.1080/0272634029008406 7

Domain Product Technique Solution for Scattering by Cylindrical Obstacle in Rectangular Waveguide

VITALIY P. CHUMACHENKO
IGOR V. PETRUSENKO

Gebze Institute of Technology
Gebze, Turkey

The canonical problem of scattering by a cylindrical obstacle in a rectangular waveguide is rigorously reexamined in the framework of the domain product technique. An accurate, rapidly converging algorithm is based on the efficient series representation of the field in a rectangular interaction region. It is shown that the fast convergence of the numerical approximation is stipulated by mathematical properties of the matrix operator arising from the boundary value formulation. The solution is also validated by comparison with the data of other authors. The approach proposed can be applied to the analysis of scattering by real metallic or dielectric posts placed parallel to the narrow or broad wall of the guide, in the theory of the circular-rectangular coaxial waveguide and the theory of other structures containing circular obstacles in the rectangular coupling region.

Keywords inductive post, waveguide discontinuities, domain product technique

Introduction

The problem of electromagnetic wave scattering by cylindrical obstacles in a rectangular waveguide has been treated by a variety of methods. An earlier approach, proposed by J. Schwinger (Schwinger & Saxon, 1968) and recently modified by Toyama and Sawado (1992), is the variational method for the problem of perfectly conducting (PEC) posts. It was proved that the elements of the impedance/admittance matrix are stationary with respect to small variations of the current distribution on the post about the true current. Many published papers are based on the so-called Rayleigh hypothesis (see, for example, Nielsen, 1969; Abdulnour & Marchildon, 1993; Wang, Wu, & Litva, 1997). In addition to the validity problem of the hypothesis, we observe that the technique usually leads to the ill-conditioned matrix equation of the first kind. As a consequence, results are

Received 3 April 2001; accepted 3 August 2001.
This research was conducted while both authors were visiting the Electronics Engineering Department, Gebze Institute of Technology, Gebze, Kocaeli, Turkey, on leave from the Zaporizhzhya National Technical University and the Dnipropetrovs'k National University, Ukraine.
Address correspondence to Igor V. Petrushenko, Electronics Engineering Department, Gebze Institute of Technology, Cayirova Kampus, P.O. 141 41400 Gebze/Kogaeli, Turkey. E-mail: petrus@penta.gyte.edu.tr

unstable with increasing the number of modes retained in the resulting algebraic system (Abdulnour & Marchildon, 1993), and the condition number may be as large as 10^{10} and over.

A multifilamentary current model was successfully applied by Leviatan et al. (1983) and Leviatan, Shau, and Adams (1984). A special approximation of the posts by a finite number of strips is used by Auda and Harrington (1984). Ise and Koshiba (1988) utilized a combination of the finite and boundary-element methods. Shunt posts in microstrip transmission lines were investigated by Finch and Alexopoulos (1990) using the multipole expansion method and the technique of the precise summation of the Schloemilch-type series. A combination of the boundary-element method and analytic expansions was applied by Abdulnour and Marchildon (1994). Commonly, data obtained are validated by computational experiment in the form of "numerical convergence" and comparative checks. A formal rigorous solution, based on the method of image and the addition theorem for cylindrical functions, was given by Moshinsky and Berezovsky (1977).

This paper presents an alternative rigorous analytical approach for solving the outlined class of problems that is quite straightforward and effective. The formulation has mathematical features that allow firm statements concerning properties of the numerical approximation. It is proved analytically that the method leads to a matrix equation of the second kind with kernel operator. That ensures the validity of the truncation procedure, the convergence of approximations to the true solution, and a stable algorithm.

In order to avoid unnecessary details, we choose the simplest possible configuration: a PEC post placed across the guide parallel to the narrow wall and parallel to the electric field of the dominant mode. To merge the circular and rectangular coordinate systems used in the analysis we also introduce an intermediate region of the form similar to that used by Nielsen (1969). However, the field is constructed in a different fashion. The region is considered as a common part (product in set-theoretic sense) of several auxiliary regions with separable geometry, and solution is based on the domain product technique (DPT) (Chumachenko, 1978). After certain manipulations, an initially somewhat cumbersome formulation is reduced to a simple algebraic system with respect to expansion coefficients that are associated with the auxiliary region related to the post. After truncation, a very small number of equations is retained in the system to guarantee a given accuracy of the solution. The computer results agree well with the published ones (Leviatan et al., 1983; Leviatan, Shau, & Adams, 1984). The method provides a reliable, rapidly converging algorithm for any finite radius and for any location of the obstacle in the interior of the guide.

Boundary Formulation and Field Representation

The configuration of interest and the coordinate systems are shown in Figure 1. A PEC post of a radius r is centered at a distance d from the narrow wall of the waveguide. The width of the guide is $2a$. The convention of time dependence is $e^{j\omega t}$. The dominant mode, of a unit amplitude, is incident from the left. The geometry is a two-dimensional (2D) one and only the electric field has a nonvanishing y-component $u = E_y$. The u must satisfy the 2D Helmholtz equation with the homogeneous Dirichlet boundary conditions on the conducting boundaries. The interior of the guide is divided into the waveguide regions I and III, and the interaction region II.

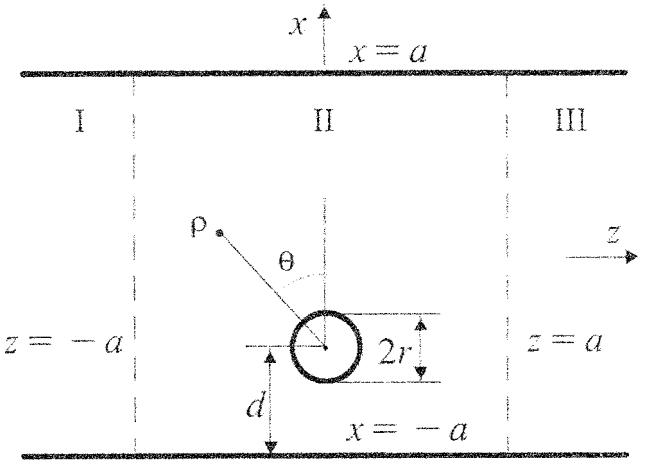

Figure 1. Geometry of the problem and pertinent coordinate systems.

Let us symbolize the field component u as $u^{(1)}$, $u^{(2)}$, and $u^{(3)}$ in regions I, II, and III correspondingly. Then, we have

$$u^{(1)} = \tau_1(x)e^{-\gamma_1(z+a)} + \sum_{n=1}^{\infty} R_n \tau_n(x) e^{\gamma_n(z+a)}, \tag{1}$$

$$u^{(3)} = \sum_{n=1}^{\infty} T_n \tau_n(x) e^{-\gamma_n(z-a)}. \tag{2}$$

Here

$$\tau_n(x) = \sin\left(\frac{n\pi(x+a)}{2a}\right), \tag{3}$$

$$\gamma_n = \sqrt{\left(\frac{n\pi}{2a}\right)^2 - k^2}, \tag{4}$$

$k = 2\pi/\lambda$, and λ is the free space wavelength. The R_n and T_n are the reflection and transmission coefficients to be found.

The Helmholtz equation is a linear one and its solution $u^{(2)}$ can be represented in the form of a superposition of some other functions being solutions to the equation, for instance,

$$u^{(2)} = u_r + \sum_{i=1}^{4} u_i. \tag{5}$$

Let us imagine region II as a common part of several semi-infinite basic regions and suppose that they are domains of definition of the functions used in (5). Namely, let u_r, u_1, u_2, u_3, and u_4 be defined in domains $\{(\rho, \theta)\colon \rho > r, -\pi < \theta \leq \pi\}$, $\{(x, z)\colon x > -a, |z| < a\}$, $\{(x, z)\colon |x| < a, z < a\}$, $\{(x, z)\colon x < a, |z| < a\}$, and $\{(x, z)\colon |x| < a, z > -a\}$, respectively. To guarantee uniqueness of the solution, we put the

functions introduced under the condition at infinity. On the rays limiting the regions, we set the requirements that provide a desired choice of the type of the expansion for u_1, u_2, u_3, and u_4. The conditions on the parts of the boundaries terminating the auxiliary regions follow from the boundary conditions of the original problem.

Separating variables, we obtain

$$u_r = E_0 \frac{H_0^{(2)}(k\rho)}{H_0^{(2)}(kr)} + \sum_{n=1}^{\infty} (E_n \cos n\theta + F_n \sin n\theta) \frac{H_n^{(2)}(k\rho)}{H_n^{(2)}(kr)}, \tag{6}$$

where $H_n^{(2)}$ is the Hankel function and E_n, F_n are the unknown expansion coefficients. Assuming that u_2 and u_4 vanish at $x = \pm a$, we get

$$u_2 = \sum_{n=1}^{\infty} D_n^{(2)} \tau_n(x) e^{\gamma_n (z-a)}, \tag{7}$$

$$u_4 = \sum_{n=1}^{\infty} D_n^{(4)} \tau_n(x) e^{-\gamma_n (z+a)}. \tag{8}$$

The u_1 and u_3 assume the form

$$u_1 = \sum_{n=0}^{\infty} D_n^{(1)} \quad {}_n(z) e^{-\gamma_n (x+a)}, \tag{9}$$

$$u_3 = \sum_{n=0}^{\infty} D_n^{(3)} \quad {}_n(z) e^{\gamma_n (x-a)}, \tag{10}$$

$${}_n(z) = \cos \frac{n\pi(z+a)}{2a}, \tag{11}$$

under qualification $\partial u_1/\partial z = \partial u_3/\partial z = 0$ at $z = \pm a$.

Now, boundary conditions on the conducting parts of the boundaries of the region II can be written as

$$u_r + u_1 + u_3 = 0, \qquad x = \pm a, \tag{12}$$

$$u_r + \sum_{i=1}^{4} u_i = 0, \qquad \rho = r. \tag{13}$$

The conditions that guarantee continuity of the tangential electric and magnetic fields across the plane $z = -a$ are given by

$$u_r + \sum_{i=1}^{4} u_i = u^{(1)}, \qquad z = -a, \tag{14}$$

$$\frac{\partial}{\partial z}(u_r + u_2 + u_4) = \frac{\partial u^{(1)}}{\partial z}, \qquad z = -a. \tag{15}$$

Similar relations are valid at $z = a$.

There are no doubts about the validity of such a representation of the field in region II. On the one hand, expression (5), constructed in the above fashion, is a solution to the Helmholtz equation inside the region. On the other hand, it provides a complete set of functions at any piece of the region boundary. The last gives an opportunity to satisfy any reasonable boundary condition.

Analyzing condition (12) and bearing in mind (6), (9), and (10), we see that $D_n^{(1)}$ and $D_n^{(3)}$ are the coefficients of the Fourier cosine series of some smooth functions. It means that $D_n^{(1)}$ and $D_n^{(3)}$ must decrease at least as $O(1/n^2)$ when n increases (Tolstov, 1976). It follows from the matching conditions at $z = \pm a$ that $D_n^{(2)}$ and $D_n^{(4)}$ are the Fourier sine coefficients of some smooth functions vanishing as $x \to \pm a$. That again leads to the estimates $D_n^{(2)}$, $D_n^{(4)} = O(1/n^2)$. At $\rho = r$, functions u_1, u_2, u_3, and u_4 are periodic with respect to θ and, being solutions to the Helmholtz equation, are differentiable an infinite number of times in the interior of their domains. Due to (6) and (13), it means that the E_n and F_n are Fourier's coefficients of a highly smooth function and must tend to zero very rapidly. Therefore, our intention is to reduce the problem to an algebraic system containing the E_n and F_n only.

Considering the Symmetry

The structure under study has a plane of symmetry $z = 0$. It can be used to sort our problem into two subproblems with the number of the unknown terms reduced to half. That is of great importance for the more effective numerical computations. We represent the solution as a sum of two solutions corresponding to the symmetric and antisymmetric excitations. We mark the related quantities by superscripts "s" and "a" if their values change. In the first case, we obtain

$$ {}^{s}u^{(1)} = \frac{1}{2}\tau_1(x)e^{-\gamma_1(z+a)} + \sum_{n=1}^{\infty} {}^{s}R_n\tau_n(x)e^{\gamma_n(z+a)}, \tag{16} $$

$$ {}^{s}u^{(3)} = \frac{1}{2}\tau_1(x)e^{\gamma_1(z-a)} + \sum_{n=1}^{\infty} {}^{s}R_n\tau_n(x)e^{-\gamma_n(z-a)}, \tag{17} $$

$$ {}^{s}F_n = {}^{s}D_{2n-1}^{(1)} = {}^{s}D_{2n-1}^{(3)} = 0, \tag{18} $$

$$ {}^{s}D_n^{(4)} = {}^{s}D_n^{(2)}. \tag{19} $$

In the antisymmetric case, we have

$$ {}^{a}u^{(1)} = \frac{1}{2}\tau_1(x)e^{-\gamma_1(z+a)} + \sum_{n=1}^{\infty} {}^{a}R_n\tau_n(x)e^{\gamma_n(z+a)}, \tag{20} $$

$$ {}^{a}u^{(3)} = -\frac{1}{2}\tau_1(x)e^{\gamma_1(z-a)} - \sum_{n=1}^{\infty} {}^{a}R_n\tau_n(x)e^{-\gamma_n(z-a)}, \tag{21} $$

$$ {}^{s}E_n = {}^{a}D_{2n}^{(1)} = {}^{a}D_{2n}^{(3)} = 0, \tag{22} $$

$$ {}^{a}D_n^{(4)} = -{}^{a}D_n^{(2)}. \tag{23} $$

Algebraization

In what follows, we consider both types of excitation simultaneously. Designations

$$o = \begin{Bmatrix} s \\ a \end{Bmatrix}, \quad \alpha = \begin{Bmatrix} 2m \\ 2m-1 \end{Bmatrix}, \quad \beta = \begin{Bmatrix} 2n \\ 2n-1 \end{Bmatrix}, \quad \tau = \begin{Bmatrix} 0 \\ 1 \end{Bmatrix},$$
$$\eta = \begin{Bmatrix} +1 \\ -1 \end{Bmatrix}, \quad A_n = \begin{Bmatrix} E_n \\ F_n \end{Bmatrix}, \quad c_n(\theta) = \begin{Bmatrix} \cos n\theta \\ \sin n\theta \end{Bmatrix}, \tag{24}$$

where the upper and lower symbols are connected with the symmetric and antisymmetric case, respectively, will make mathematical manipulations less cumbersome. We start with the substitution (6), (9), and (10) into (12). The resulting equations are then multiplied on each side with $_\alpha$ and integrated over z. Considering (18), (19), (22), (23) and making use of the orthogonality of the $_\alpha$ functions, we get

$$D_\alpha^{(1)} + D_\alpha^{(3)} e^{-2\gamma_\alpha a} + \sum_{n=\tau}^{\infty} d_{\alpha n}^{-} A_n = 0, \tag{25}$$

$$D_\alpha^{(1)} e^{-2\gamma_\alpha a} + D_\alpha^{(3)} + \sum_{n=\tau}^{\infty} d_{\alpha n}^{+} A_n = 0, \tag{26}$$

where

$$d_{\alpha n}^{\pm} = \frac{2}{\varepsilon_m a} \int_0^a \left[c_n(\theta) \frac{H_n^{(2)}(k\rho)}{H_n^{(2)}(kr)} \right]_{x=\pm a} {}_\alpha(z) dz, \tag{27}$$

$$\varepsilon_m = 2, \quad m = 0, \quad \varepsilon_m = 1, \quad m \geq 1. \tag{28}$$

Expression (27) has been written, taking into account the evenness of the integrand with respect to z. Combining equations (25) and (26), we find

$$D_\alpha^{(1)} = \sum_{n=\tau}^{\infty} \tilde{d}_{\alpha n} A_n, \qquad D_\alpha^{(3)} = \sum_{n=\tau}^{\infty} \hat{d}_{\alpha n} A_n, \tag{29}$$

where

$$\tilde{d}_{\alpha n} = t_\alpha (d_{\alpha n}^{-} - e^{-2\gamma_\alpha a}\, d_{\alpha n}^{+}), \tag{30}$$

$$\hat{d}_{\alpha n} = t_\alpha (d_{\alpha n}^{+} - e^{-2\gamma_\alpha a}\, d_{\alpha n}^{-}), \tag{31}$$

$$t_\alpha = 1/(e^{-4\gamma_\alpha a} - 1). \tag{32}$$

The use of the matching conditions (14) and (15) yields after similar manipulations

$${}^{o}D_m^{(2)} = \frac{\eta}{2} \left\{ \sum_{n=\tau}^{\infty} [q_{m\beta}^{(1)} D_\beta^{(1)} + q_{m\beta}^{(3)} D_\beta^{(3)} + ({}^{o}q_{mn}^{(4)} - {}^{o}f_{mn}) A_n] + \delta_{1m} \right\}, \tag{33}$$

$${}^{o}R_m = \frac{\eta}{2} \left\{ \sum_{n=\tau}^{\infty} [e_m^{\mp} (q_{m\beta}^{(1)} D_\beta^{(1)} + q_{m\beta}^{(3)} D_\beta^{(3)}) + (e_m^{\mp}\, {}^{o}q_{mn}^{(4)} - e_m^{\pm}\, {}^{o}f_{mn}) A_n] + \delta_{1m} e^{-2\gamma_1 a} \right\}. \tag{34}$$

Here

$$e_m^{\pm} = e^{-2\gamma_m a} \pm 1, \tag{35}$$

$$q_{m\beta}^{(1)} = \frac{m\pi}{2a^2}[(-1)^m e^{-2\gamma_\beta a} - 1] \Bigg/ \left[\gamma_\beta^2 + \left(\frac{m\pi}{2a}\right)^2\right], \tag{36}$$

$$q_{m\beta}^{(3)} = (-1)^{m+1} q_{m\beta}^{(1)}, \tag{37}$$

$${}^o q_{mn}^{(4)} = -\frac{1}{a}\int_{-a}^{a}\left[c_n(\theta)\frac{H_n^{(2)}(k\rho)}{H_n^{(2)}(kr)}\right]_{z=-a}\tau_m(x)dx, \tag{38}$$

$${}^o f_{mn} = -\frac{1}{a\gamma_m}\int_{-a}^{a}\frac{\partial}{\partial z}\left[c_n(\theta)\frac{H_n^{(2)}(k\rho)}{H_n^{(2)}(kr)}\right]_{z=-a}\tau_m(x)dx. \tag{39}$$

In (34), the upper plus or minus corresponds to the symmetric excitation, and the lower to the antisymmetric one. Next, we substitute (29) into (33) to express ${}^s D_m^{(2)}$ and ${}^a D_m^{(2)}$ in terms of E_n and F_n. We have

$${}^o D_m^{(2)} = \sum_{i=\tau}^{\infty} {}^o a_{mi} A_i + \frac{\eta}{2}\delta_{1m} \tag{40}$$

with

$${}^o a_{mi} = \frac{\eta}{2}\left[\sum_{n=\tau}^{\infty}(q_{m\beta}^{(1)}\tilde{d}_{\beta i} + q_{m\beta}^{(3)}\hat{d}_{\beta i}) + {}^o q_{mi}^{(4)} - {}^o f_{mi}\right]. \tag{41}$$

Substituting (6)–(10) into (13) and working as before, we arrive at

$$\sum_{n=\tau}^{\infty} p_{m\beta}^{(1)} D_\beta^{(1)} + \sum_{n=1}^{\infty} {}^o p_{mn}^{(2)} {}^o D_n^{(2)} + \sum_{n=\tau}^{\infty} p_{m\beta}^{(3)} D_\beta^{(3)} + A_m = 0, \tag{42}$$

where

$$p_{m\beta}^{(1)} = \frac{2}{\varepsilon_m \pi}\int_0^{\pi}[\ \ _\beta(z)e^{-\gamma_\beta(x+a)}]_{\rho=r} c_m(\theta)d\theta, \tag{43}$$

$${}^o p_{mn}^{(2)} = \frac{2}{\varepsilon_m \pi}\int_0^{\pi}[(e^{\gamma_n(z-a)} + \eta e^{-\gamma_n(z+a)})\tau_n(x)]_{\rho=r} c_m(\theta)d\theta, \tag{44}$$

$$p_{m\beta}^{(3)} = \frac{2}{\varepsilon_m \pi}\int_0^{\pi}[\ \ _\beta(z)e^{\gamma_\beta(x-a)}]_{\rho=r} c_m(\theta)d\theta. \tag{45}$$

Finally, using (29) and (40), we eliminate $D_\beta^{(1)}$, ${}^o D_n^{(2)}$, and $D_\beta^{(3)}$ in (42). That gives us two uncoupled infinite systems with respect to E_n and F_n:

$$E_m + \sum_{i=0}^{\infty} {}^s b_{mi} E_i = -\frac{1}{2} {}^s p_{m1}^{(1)}, \tag{46}$$

$$F_m + \sum_{i=1}^{\infty} {}^a b_{mi} F_i = \frac{1}{2} {}^a p_{m1}^{(1)}, \tag{47}$$

where

$$ {}^{o}b_{mi} = \sum_{n=\tau}^{\infty} (p_{m\beta}^{(1)} \tilde{d}_{\beta i} + p_{m\beta}^{(3)} \hat{d}_{\beta i}) + \sum_{n=1}^{\infty} {}^{o}p_{mn}^{(2)} {}^{o}a_{ni}. \tag{48} $$

In the matrix form both (46) and (47) can be rewritten as

$$ (I + {}^{o}B)A = {}^{o}g, \tag{49} $$

where I is an identity, ${}^{o}B = \{{}^{o}b_{mi}\}$, $A = \{A_m\}$, and ${}^{o}g = -\frac{\eta}{2}\{{}^{o}p_{m1}^{(1)}\}$. Matrix ${}^{o}B$ presents the so-called kernel operator (the details are given in the appendix). This fact guarantees, in particular, (a) the boundedness of the inverse matrix operator for equations (46) and (47), (b) the validity of the truncation procedure, and (c) the convergence of approximations to the true solution.

On truncating systems (46) and (47) and subsequent inverting, the E_n and F_n are found. Other expansion coefficients can be obtained using (29), (34), and (40). Integrals (27), (38), (39), and (43)–(45) are conveniently computed based on numerical techniques. For terminal planes $z = 0\pm$, the elements of the scattering matrix are given by

$$ S_{11} = S_{22} = ({}^{s}R_1 + {}^{a}R_1)e^{2\gamma_1 a}, \tag{50} $$

$$ S_{12} = S_{21} = ({}^{s}R_1 - {}^{a}R_1)e^{2\gamma_1 a}. \tag{51} $$

For operation frequency between the cutoffs of the TE_{10} and TE_{20} modes, the normalized parameters of an equivalent T-circuit of the discontinuity can be found as

$$ X = -j2S_{21}/[(1 - S_{11})^2 - S_{21}^2], \tag{52} $$

$$ Y = j(1 + S_{11} - S_{21})/(1 - S_{11} + S_{21}). \tag{53} $$

Numerical Validation

In this section, we present numerical results that validate the theory developed and illustrate its efficiency. Let M be max n in (6) and $N = \max\ n$ in (1), (2), and (7)–(10) after truncation. M also determines the order of the truncated systems (46) and (47). Table 1 illustrates convergence of the algorithm. Last decimals are rounded. The rate of stabilization of the data obtained is extremely high with respect to M. In the range of the post dimensions, encountered commonly in practice, it is enough to use $M = 1 \div 3$, $N = 5$ in systems (46) and (47) to achieve accuracy sufficient for engineering needs. In the last two sections of Table 1, data are presented that characterize the unitary property of the S-matrix. Despite the fact that the unitary condition is not an entirely adequate tool for the accuracy evaluation (Shestopalov, Kirilenko, & Masalov, 1984), they also confirm the validity of the solution.

In Figure 2, the calculated values of the reactances are compared with the data obtained by Leviatan et al. (1983). They completely agree with our results within drawing precision. Figure 3 shows the real parts of currents induced on the post that have known counterparts (Leviatan, Shau, & Adams, 1984). Some discrepancies, which are most conspicuous for small values of the r/a ratio, are due to the multifilamentary model.

The performed numerical investigation and the established properties of the matrix operator turn the algorithm into a reliable tool for comparative checks. For the post centered in the waveguide, we have solved the above problem using the Rayleigh hypothesis,

Table 1
Dependencies of the S-matrix elements on the truncation numbers M, N, and the geometrical parameters d and r for $a/\lambda = 0.35$ ($PCL = |S_{11}|^2 + |S_{21}|^2$, $ORT = S_{11}\overline{S}_{21} + S_{12}\overline{S}_{22}$).

$d/a = 0.2$, $r/a = 0.1$, $N = 40$				
M	$\lvert S_{11}\rvert$	arg S_{11}	$\lvert S_{21}\rvert$	arg S_{21}
1	0.152444	1.733263	0.988312	0.162469
2	0.152111	1.733836	0.988364	0.163042
5	0.152112	1.733837	0.988364	0.163043
10	0.152112	1.733837	0.988364	0.163043
$d/a = 0.2$, $r/a = 0.1$, $M = 5$				
N	$\lvert S_{11}\rvert$	arg S_{11}	$\lvert S_{21}\rvert$	arg S_{21}
1	0.146147	1.693725	0.994160	0.156507
2	0.149397	1.715330	0.991045	0.159842
5	0.151931	1.733987	0.988333	0.162818
10	0.152108	1.733713	0.988382	0.163035
20	0.152111	1.733826	0.988366	0.163042
40	0.152112	1.733837	0.988364	0.163043
$d/a = 0.6$, $r/a = 0.5$, $N = 40$				
M	$\lvert S_{11}\rvert$	arg S_{11}	$\lvert S_{21}\rvert$	arg S_{21}
1	0.999311	−2.190575	0.037108	2.521810
2	0.999028	−2.124246	0.044067	2.588141
3	0.999152	−2.117523	0.041164	2.594864
5	0.999146	−2.117144	0.041296	2.595242
10	0.999146	−2.117143	0.041297	2.595244
20	0.999146	−2.117143	0.041297	2.595244
$d/a = 0.6$, $r/a = 0.5$, $M = 10$				
N	$\lvert S_{11}\rvert$	arg S_{11}	$\lvert S_{21}\rvert$	arg S_{21}
1	0.977358	−2.097857	0.022178	1.868905
2	0.994023	−2.122385	0.031834	2.624531
5	0.998931	−2.117037	0.041010	2.593123
10	0.999113	−2.117145	0.041252	2.595188
20	0.999142	−2.117142	0.041292	2.595230
40	0.999146	−2.117143	0.041297	2.595244

(*continued*)

Table 1
(*Continued*)

$d/a = 1,\ r/a = 0.9,\ N = 40$				
M	$\lvert S_{11}\rvert$	arg S_{11}	*PCL*	*ORT*
1	0.992999	−0.758778	0.999998	0.000001
2	0.999072	−0.597320	0.999999	0.000002
3	0.999952	−0.544489	0.999999	0.000002
4	0.999999	−0.533255	0.999999	0.000002
5	1.000000	−0.531709	0.999999	0.000002
10	1.000000	−0.531633	0.999999	0.000002
20	1.000000	−0.531633	0.999999	0.000002
$d/a = 1,\ r/a = 0.9,\ M = 10$				
N	$\lvert S_{11}\rvert$	arg S_{11}	*PCL*	*ORT*
1	0.992604	−0.522419	0.986193	0.028824
2	0.993057	−0.534606	0.986602	0.029233
5	0.999941	−0.531618	0.999882	0.000666
10	0.999976	−0.531647	0.999952	0.000092
20	0.999997	−0.531634	0.999994	0.000012
40	1.000000	−0.531633	0.999999	0.000002

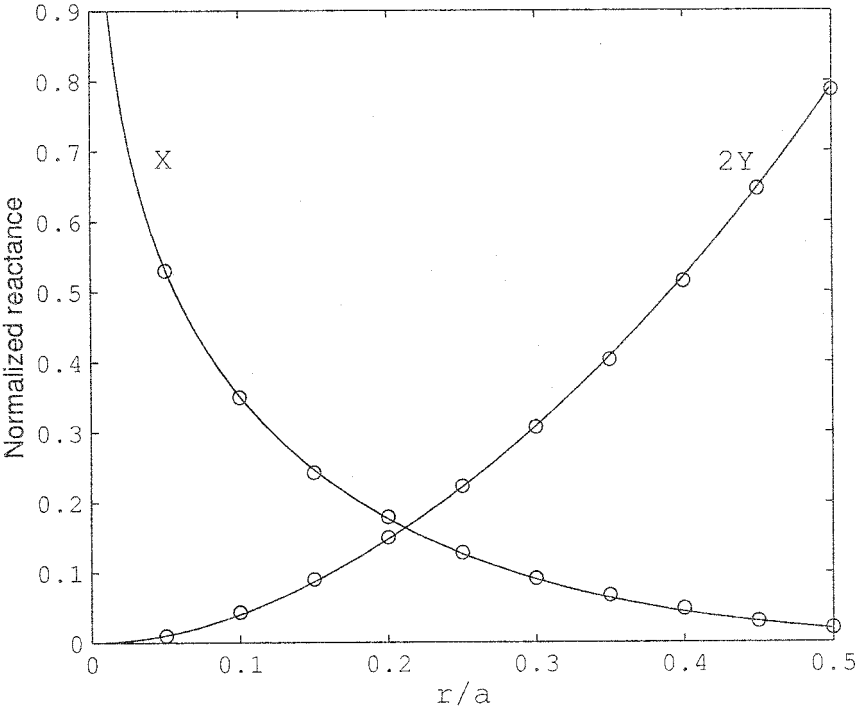

Figure 2. Circuit parameters versus r/a for $d/a = 0.6$ and $a/\lambda = 0.3571$. Solid lines: this technique; circles: data from Leviatan et al., 1983.

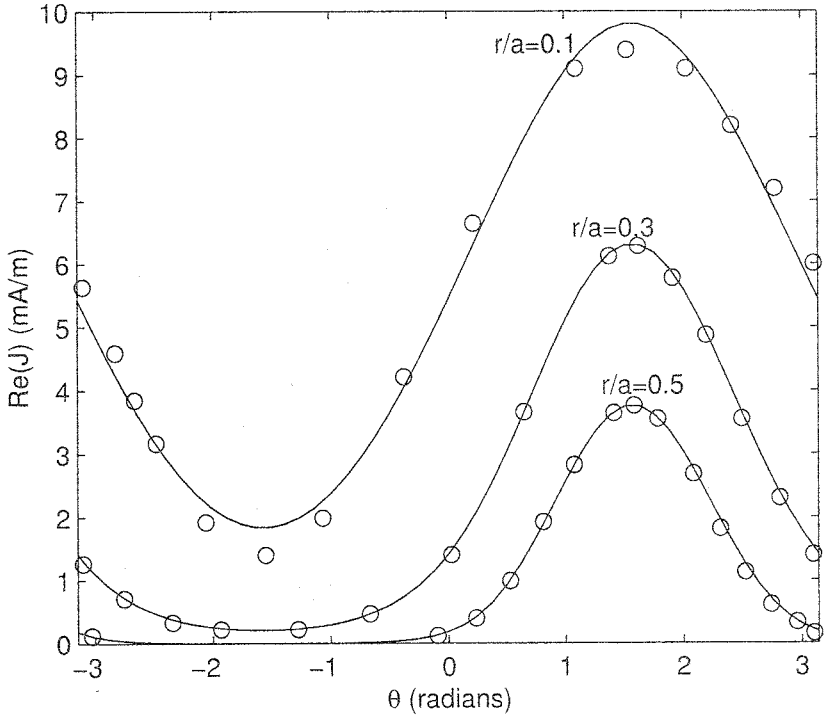

Figure 3. Real part of current versus θ for $d/a = 1$ and $a/\lambda = 0.4167$. Solid lines: this technique; circles: data from Leviatan, Shan & Adams, 1984.

just as was done by Abdulnour and Marchildon (1993). To reduce the condition number and intensify the efficiency of the computational procedure, the problem was separated in the above manner into two subproblems for the symmetric and antisymmetric excitations. The results obtained lend support to the validity of the Rayleigh hypothesis. In spite of the extremely high condition number, the agreement was fairly good in a wide frequency range for both small and larger posts. Figure 4 shows typical behavior of the maximums of the condition numbers for two methods discussed. In each case, we cite the greater value found for two subproblems in the numerical process.

Conclusion

The problem of the scattering of electromagnetic waves by a single cylindrical obstacle in a rectangular waveguide is formulated in the framework of the DPT. The problem is reduced to two independent linear systems with respect to the coefficients of the expansion associated with the post. Analytical study has shown that matrix operators that occur in the solution possess remarkable properties. As a consequence, the systems can be efficiently solved numerically. The high-accuracy values of the scattering matrix and the parameters of the equivalent circuit are determined with low computational cost in the entire range $0 < r < a$. The data, excellent for any engineering needs, can be found with an extremely small number of equations retained after truncation. The computed results show good agreement with the data obtained by other authors.

After obvious modification, the approach developed can be used for analysis of scattering by one or several real dielectric or metallic posts placed in a rectangular

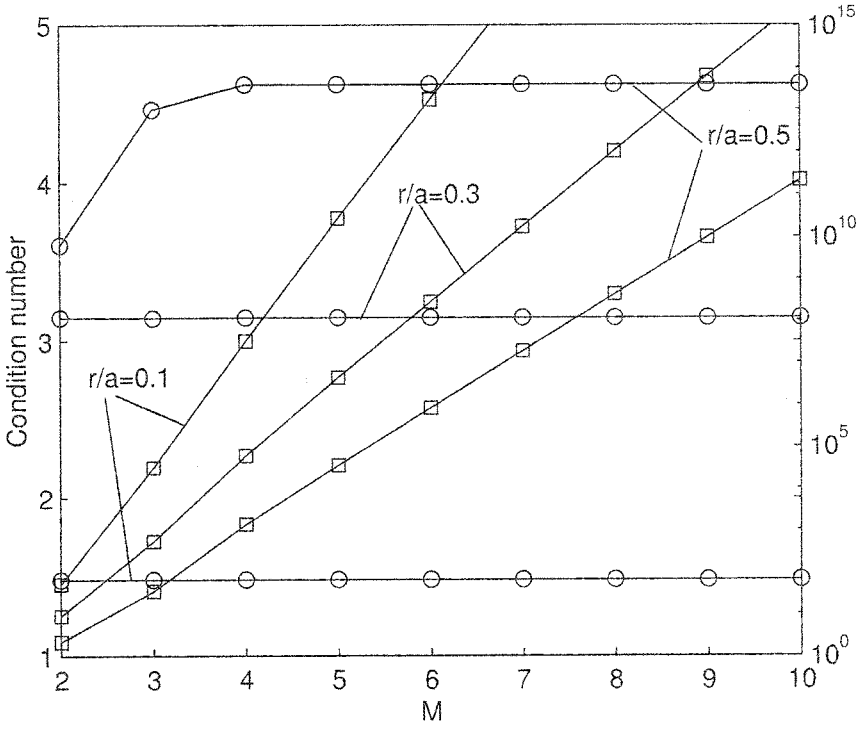

Figure 4. Condition number versus number of equations retained after truncation for $d/a = 1$ and $a/\lambda = 0.8$. Circles: this technique ($N = 40$, left-hand linear axis); squares: technique based on Rayleigh hypothesis (right-hand logarithmic axis).

waveguide parallel to the narrow or broad wall. It can also be applied in the theory of the circular-rectangular waveguide. Similar ideas can be used in the analysis of the H- or E-plane waveguide junctions (such as, for example, T- or cross-junction) with posts in connecting cavity. The high-accuracy numerical data, given in the previous section, can serve in testing computations with more general geometry.

Appendix

Because

$$A \in \tilde{\ell}_2, \qquad \tilde{\ell}_2 \equiv \left\{ x_n : \sum_{n=1}^{\infty} n|x_n|^2 < \infty \right\},$$

(Shestopalov, Kinilenko, & Masalov, 1984) it is convenient to change A and ${}^o g$ for

$$\tilde{A} \equiv \{n^{1/2} A_n\} \in \ell_2 \quad \text{and} \quad {}^o\tilde{g} \equiv \left\{ m^{1/2} \frac{-\eta}{2} {}^o p_{m1}^{(1)} \right\}.$$

It can be readily verified that ${}^o\tilde{g} \in \ell_2$ as well. Let us rewrite the matrix operator in (49) in the form

$${}^o\tilde{B} = \left(P_1 + \frac{\eta}{2} {}^o W Q_1 \right) \tilde{L} + \left(P_3 + \frac{\eta}{2} {}^o W Q_3 \right) \hat{L} + {}^o W ({}^o G - {}^o F),$$

where the matrices introduced are defined as follows:

$$P_i \equiv \{m^{1/2} p_{mn}^{(i)}\}, \quad {}^{o}W \equiv \{(mn)^{1/2} {}^{o}p_{mn}^{(2)}\}, \quad Q_i \equiv \{m^{-1/2} q_{mn}^{(i)}\}, \quad i = 1, 3;$$

$$\tilde{L} \equiv \{n^{-1/2} \tilde{d}_{mn}\}, \quad \hat{L} \equiv \{n^{-1/2} \hat{d}_{mn}\}, \quad {}^{o}G \equiv \{(mn)^{-1/2} \, {}^{o}q_{mn}^{(4)}\}, \quad {}^{o}F \equiv \{(mn)^{-1/2} \, {}^{o}f_{mn}\}.$$

With the help of Parseval's theorem, we find that

$$\sum_{m,n} \frac{1}{n} |d_{mn}^{\pm}|^2 < \infty, \quad \sum_{m,n} \frac{1}{mn} |{}^{o}q_{mn}^{(4)}|^2 < \infty, \quad \sum_{m,n} \frac{1}{mn} |{}^{o}f_{mn}|^2 < \infty$$

for any possible radius of the post. Hence, $\tilde{L}$, $\hat{L}$, G, and F are the Hilbert–Schmidt (H–S) operators $\ell_2 \to \ell_2$ (Reed & Simon, 1972).

As to matrices P_i, $i = 1, 3$, and ${}^{o}W$ for $n \gg 1$ the integrals (43)–(45) can be reduced to the known ones (Gradshteyn & Ryzhik, 1994, (3.932)) and we obtain

$$\sum_{m,n} m |p_{mn}^{(i)}|^2 = O[(1 - v_i)^{-\alpha}, \quad \alpha > 0, \quad i = 1, 3;$$

$$\sum_{m,n} mn |{}^{o}p_{mn}^{(2)}|^2 = O[(1 - v_2)^{-\beta}], \quad \beta > \alpha > 0,$$

where

$$\vec{v} \equiv \left(\frac{r}{d}, \frac{r}{a}, \frac{r}{2a - d} \right).$$

Therefore, the P_i, $i = 1, 3$, and ${}^{o}W$ also present the H–S operators provided the post does not touch the boundaries of the interaction region II. Finally, owing to

$$\sum_{m,n} \frac{1}{m} |q_{mn}^{(i)}|^2 < \infty,$$

the same holds for matrices Q_i, $i = 1, 3$.

Thus, matrix operator ${}^{o}\tilde{B} : \ell_2 \to \ell_2$ is the kernel operator (as a sum of products of the H–S operators) and the analytical Fredholm alternative is valid for the resulting system (49) (Reed & Simon, 1972).

References

Abdulnour, J., & L. Marchildon. 1993. Scattering by a dielectric obstacle in a rectangular waveguide. *IEEE Trans. Microwave Theory Tech.* 41:1988–1994.

Abdulnour, J., & L. Marchildon. 1994. Boundary elements and analytic expansions applied to H-plane waveguide junctions. *IEEE Trans. Microwave Theory Tech.* 42:1038–1045.

Auda, H., & R. F. Harrington. 1984. Inductive posts and diaphragms in a rectangular waveguide. *IEEE Trans. Microwave Theory Tech.* 32:606–613.

Chumachenko, V. P. 1978. The use of integral equation method for solving one class of electrodynamics problems. *Izvestiya VUZ. Radiofizika* 21:1004–1010 (in Russian).

Finch, K. L., & N. G. Alexopoulos. 1990. Shunt posts in microstrip transmission lines. *IEEE Trans. Microwave Theory Tech.* 38:1585–1594.

Gradshteyn, I. S., and I. M. Ryzhik. 1994. *Table of Integrals, Series, and Products*, 5th ed. New York: Academic Press.

Ise, K., & M. Koshiba. 1988. Numerical analysis of H-plane waveguide junctions by combination of finite and boundary elements. *IEEE Trans. Microwave Theory Tech.* 36:1343–1351.

Leviatan, Y., P. G. Li, A. T. Adams, & J. Perini. 1983. Single-post inductive obstacle in rectangular waveguide. *IEEE Trans. Microwave Theory Tech.* 31:806–812.

Leviatan, L., D. H. Shau, & A. T. Adams. 1984. Numerical study of the current distribution on a post in a rectangular waveguide. *IEEE Trans. Microwave Theory Tech.* 32:1411–1415.

Moshinsky, A. V., & V. K. Berezovsky. 1977. Rigorous solution of the H_{10} wave scattering problem on the cylindrical discontinuity in a rectangular waveguide. *Radiotekhnika i Elektronika* 22:1350–1354 (in Russian).

Nielsen, E. D. 1969. Scattering by a cylindrical post of complex permittivity in a waveguide. *IEEE Trans. Microwave Theory Tech.* 17:148–153.

Reed, M., and B. Simon. 1972. *Methods of modern mathematical physics, V. 1. Functional analysis.* New York: Academic Press.

Schwinger, J., & D. S. Saxon. 1968. *Discontinuities in waveguide.* New York: Gordon and Breach.

Shestopalov, V. P., A. A. Kirilenko, & S. A. Masalov. 1984. *Convolution-type matrix equations in the theory of diffraction.* Kyiv: Naukova Dumka (in Russian).

Tolstov, G. P. 1976. *Fourier series.* New York: Dover.

Toyama, T., & E. Sawado. 1992. Functionals in the variational method applied to equivalent impedance matrix of metallic posts unsymmetrically positioned in a rectangular waveguide. *IEEE Trans. Microwave Theory Tech.* 40:1655–1660.

Wang, H., K.-L. Wu, & J. Litva. 1997. The higher order modal characteristics of circular-rectangular coaxial waveguides. *IEEE Trans. Microwave Theory Tech.* 45:414–419.